Available online at www.sciencedirect.com
SCIENCE DIRECT®
Journal of Solid State Chemistry 178 (2005) 2436–2451
JOURNAL OF SOLID STATE CHEMISTRY
www.elsevier.com/locate/jssc

Soft functional polynuclear coordination compounds containing pyrimidine bridges

Jorge A.R. Navarro[a,*], Elisa Barea[a], Miguel A. Galindo[a], Juan M. Salas[a], M. Angustias Romero[a], Miguel Quirós[a], Norberto Masciocchi[b,**], Simona Galli[b], Angelo Sironi[c], Bernhard Lippert[d,***]

[a]*Departamento de Química Inorgánica, Universidad de Granada, Av. Fuentenueva S/N, 18071 Granada, Spain*
[b]*Dipartimento di Scienze Chimiche e Ambientali, Università dell'Insubria, Via Valleggio 11, 22100 Como, Italy*
[c]*Dipartimento di Chimica Strutturale e Stereochimica Inorganica, Università di Milano and Istituto di Scienze e Tecnologie Molecolari del CNR (ISTM-CNR), Via Venezian 21, 20133 Milano, Italy*
[d]*Fachbereich Chemie. Universität Dortmund, Otto-Hahn-Strasse 6, D-44221 Dortmund, Germany*

Received 8 February 2005; accepted 13 May 2005
Available online 29 June 2005

Abstract

In this account, we describe the use of simple pyrimidine derivatives in combination with metal ions to build highly structured molecular architectures containing functional nanoenvironments, cavities and surfaces that can interact with additional species. The supramolecular structure of these systems can be rationally controlled by metal fragment geometry, reaction conditions and presence of templating agents. Thus, the use of transition metals with low coordination numbers or blocked bonding positions in combination with pyrimidines (e.g. 2-hydroxypyrimidine, 4-hydroxypyrimidine, 2,4-dihydroxypyrimidine, 2-aminopyrimidine) leads to the formation of either discrete assemblies, 1D polymers or helixes. When metal ions with higher coordination possibilities are applied instead, 2D and 3D networks are generated. Some of the assemblies built in this way possess functional cavities, pores and surfaces that can interact with additional species by means of hydrophobic, electrostatic, H-bonding interactions and coordinative bonds to give rise to recognition processes. The latter range from molecular recognition in homogeneous phase as well as clathrate formation, to heterogeneous solid–gas and solid–liquid adsorption phenomena. It should be noted that these materials are not rigid but able to undergo guest-induced reorganisation processes even in the solid state. Finally, some of these materials also combine additional interesting magneto-optical properties. Thus, dual systems can be envisaged in which two or more of these properties are present in the same material.

Keywords: Open metal organic frameworks; Host–guest chemistry; Supramolecular chemistry; Ion pair receptors; Solid–gas sorption; Solid–liquid sorption; Solid-to-solid reaction; Phase transition

1. Introduction

Transition metal ions have proven to be extremely important in self-assembly processes leading to discrete nano-sized species or infinite coordination polymers [1]. Small protein-sized molecules have been synthesised in this way [2], and there are numerous reports on exciting host–guest chemistry of such systems and interesting applications relevant to sensing, sieving and catalysis,

*Corresponding author. Fax: +34 95 824 85 26.
**Corresponding author. Fax: +39 031 2386119.
***Corresponding author. Fax: +49 231 755 3797.
E-mail addresses: jarn@ugr.es (J.A.R. Navarro), norberto.masciocchi@unisubria.it (N. Masciocchi), bernhard.lippert@uni-dortmund.de (B. Lippert).

0022-4596/$ - see front matter © 2005 Elsevier Inc. All rights reserved.
doi:10.1016/j.jssc.2005.05.011

among others [3]. Molecular capsules have also been used to stabilise highly reactive species (''ship-in-a-bottle'' synthetic strategies) and to carry out selective reactions in the confined space of a capsule [4].

Zeolitic nanoporous materials are of great interest in regard of their wide range of technological applications (for example acting as molecular sieves, ion exchangers, catalysts [5] and as supporters of active components [6]). Although they are chemically stable, their functionalisation and preparation, with a rigorous control of the pore size, are difficult. These materials are also limited by the implicit anionic nature of the structure framework. In addition, they lack interesting features such as homochirality or flexibility that are found in the catalytic sites of enzymes. Application of self-assembly processes of suitable building blocks of metal ions and organic ligands is an advantageous way to obtain alternative nanoporous materials [2,3,7]. In addition, this strategy not only increases the range of possible architectures due to the diverse stereochemical properties of metal ions, but also enormously expands the functional properties of these systems. For instance, the resulting materials possess the magnetic, optical, catalytic and structural properties intrinsic to metal ions [8,9] and the flexibility and functionality of the organic linkers [10,11]. Thus, very promising compounds have been developed in this way with properties ranging from the secure storage of highly reactive gases [7,11] to the development of catalysts [9,10].

1.1. Molecular architecture with metal ions and pyrimidines

Pyrimidine derivatives, in spite of their simplicity, are very versatile systems. Their ability for giving specific H-bonding patterns as a key step in the storage and transmission of genetic information is a well-known process [12]. Their efficiency in binding metal ions is also well known. Indeed, they are ideally suited for acting as bridges of two or more metal ions to give both discrete and extended polynuclear compounds [13]. Simultaneous presence of coordinative bonds and H-bonding interactions is also an advantageous way for constructing complex supramolecular assemblies [14].

The structure and dimensionality of this type of materials can be controlled from discrete to infinite 3D polymeric open-frameworks, in a rational way, by the right choice of pyrimidine functionalisation, H-bonding donor–aceptor sequences, metal fragment geometries, reaction conditions and presence of templating agents [14].

The synthetic strategy employed by us to build aggregated complexes is very simple. As shown in Fig. 1, considering only the participation of the endocyclic pyrimidine N atoms and simple metal fragment geometries or H-bonds, cyclic open boxes, planar hexagons, 1D polymeric chains or helixes and 2D or 3D extended materials can be obtained. However, it should be noted that we have employed substituted pyrimidines, which lead to additional possibilities to create materials with functionalised cavity surfaces and pores able to interact with other species. Depending on the pyrimidine functionalisation, highly specific molecular recognition processes for cationic, neutral or anionic species by means of a mixture of hydrophobic, electrostatic and H-bonding interactions and coordinative bonds are possible.

The examples described hereafter range from molecular recognition in homogeneous phase to formation of clathrates, as well as heterogeneous solid–gas and solid–liquid adsorption processes. For the latter systems, it should be noted that, in spite of their extended nature, they are not rigid but able to give guest-induced solid-to-solid-phase transitions (see below). Finally, some of these materials also combine additional interesting magneto-optical properties (see below). Thus, dual systems can be envisaged in which two or more of these properties are present in a material.

1.1.1. The pyrimidine ligands

In recent years, we have studied metal complexes formation with simple pyrimidine (pym) derivatives: 2-hydroxypyrimidine (2-Hpymo), 2-hydroxy-5-nitropyrimidine (2-Hnitropymo), 4-hydroxypyrimidine (4-Hpymo), 4,6-dimethyl-2-hydroxypyrimidine (2-Hdmpymo), uracil (UH_2), 2-aminopyrimidine (Hampym), and the pyrimidine geometrically related heterocycle 4,7-phenanthroline (4,7-Phen) (Fig. 2). We have paid special attention to the programmed construction of aggregates containing functional cavities, channels or surfaces. All these ligands are characterised by their rigid nature, the 120° disposition of the ideal bonding of the endocyclic N atoms and the possibility of additional interactions either through their exocyclic substituents or their π-surface.

1.1.2. The metals

The geometry, reaction kinetics and electronic nature of the metal ions involved in the formation of the supramolecular structure will determine the structure itself, its robustness and its functional properties. Metal ions exhibiting fast reactivity, i.e. first row divalent transition metal ions and Pd^{II}, Cd^{II}, Ag^{I} and Cu^{I}, are suited for giving efficient self-assembly processes to build well-structured supramolecular systems. The geometrical preferences of these metal ions, i.e. linear, square-planar, tetrahedral or octahedral stereochemistry or the presence of blocked coordination positions in the metal entity will also determine the type of product to be obtained. Nevertheless, in some cases, deviation from ideal angles will be an added value for the obtention of unexpected novel frameworks.

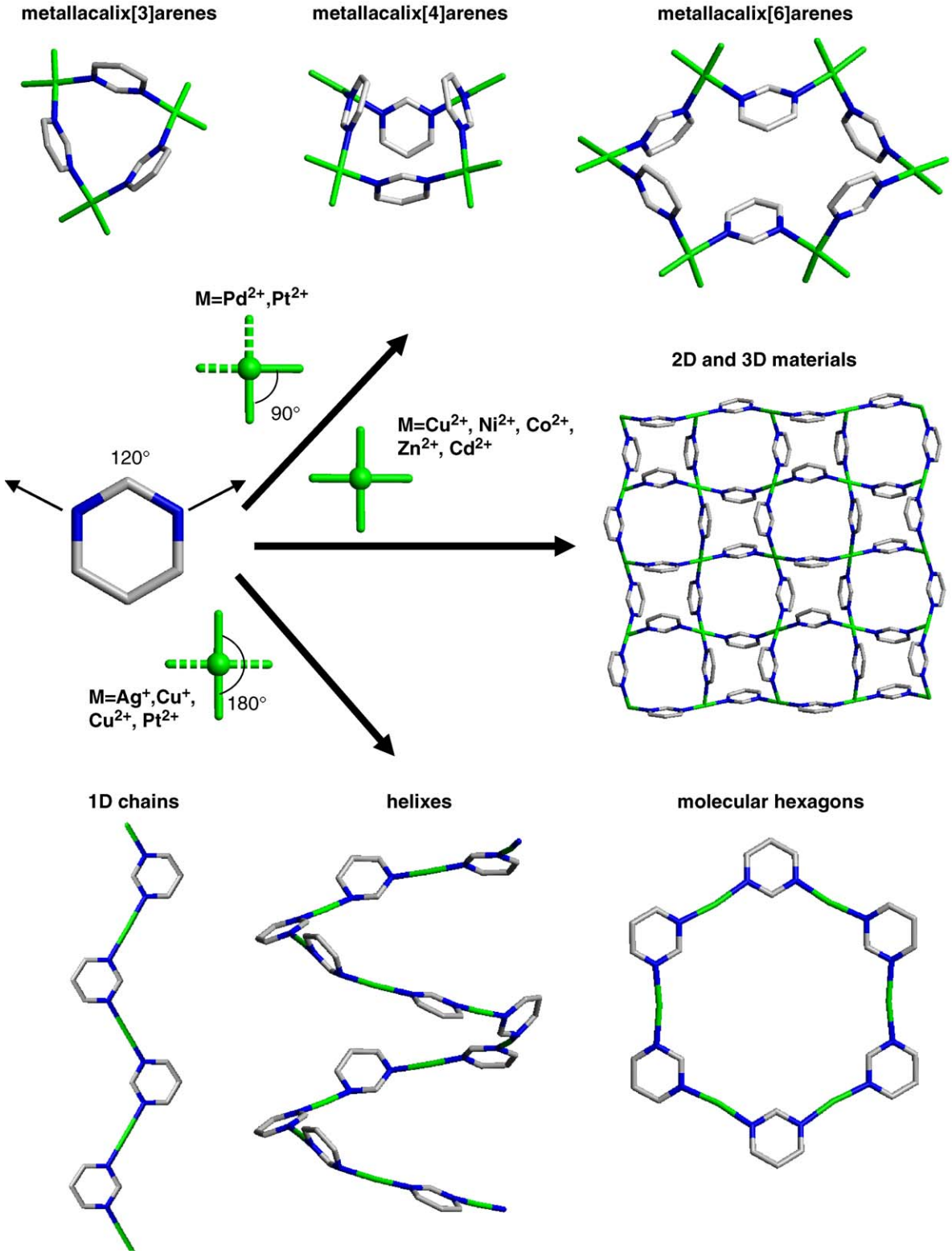

Fig. 1. Framework topologies built upon self-assembly processes involving pyrimidine moieties and metal fragments of different geometric requirements.

Another interesting feature of the systems reported here is that, in spite of the rigid nature of the bridging ligands, they are conformationally flexible even in the case of extended compounds, due to the possibility of rotation about the metal–N atom bonds. In the following, selected examples originated from our work

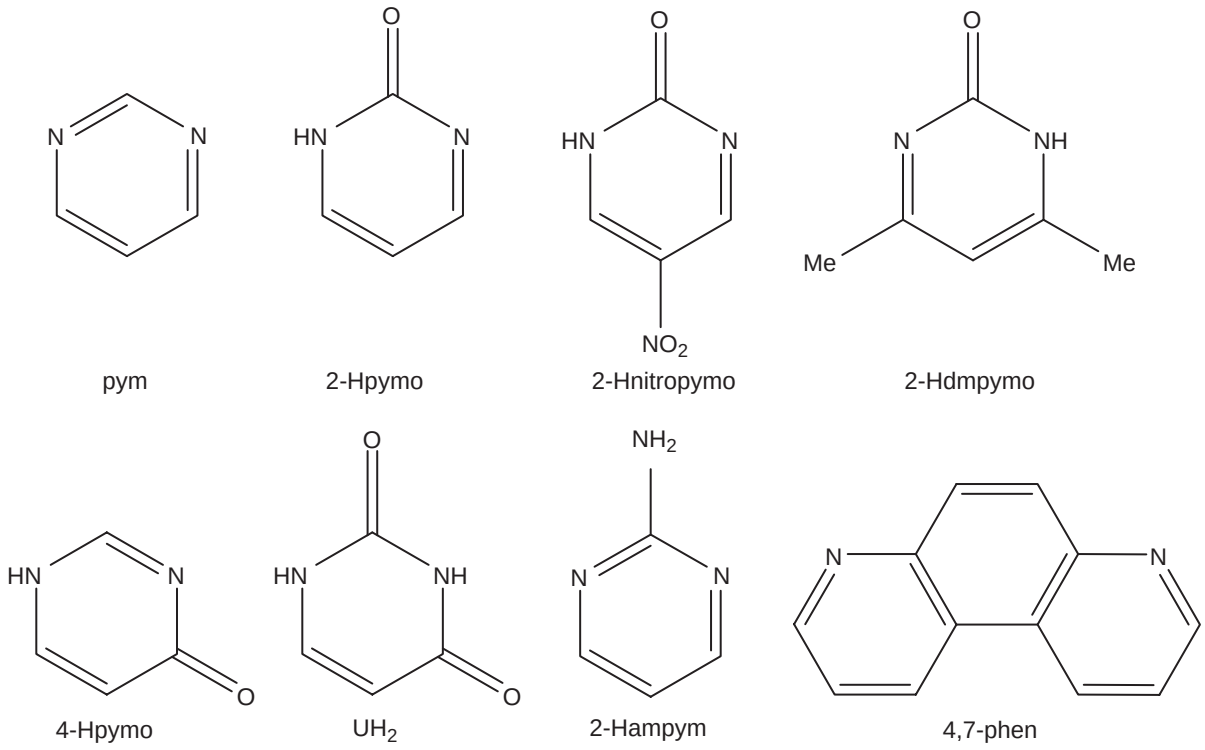

Fig. 2. Pyrimidine (pym), 2-hydroxypyrimidine (2-Hpymo), 2-hydroxy-5-nitropyrimidine (2-Hnitropymo), 4,6-dimethyl-2-hydroxypyrimidine (2-Hdmpymo), 4-hydroxypyrimidine (4-Hpymo), uracil (UH_2), 2-aminopyrimidine (2-ampym), 4,7-phenanthroline (4,7-Phen).

will be presented and discussed. As it will be pointed out, the high affinity of some of these ligands for more than just one metal ion frequently leads to supramolecular entities that are rich in metal ions, nevertheless, these materials not always are highly charged.

2. Metallacalixarenes. *Cis* geometry of the metal

2.1. Metallacalixarenes built of pyrimidine ligands

2.1.1. Uracil metallacalix[4]arenes

We have shown that the *cis* blocked metal entity $[Pt(en)Cl_2]$ reacts with unsubstituted uracil (UH_2) to give *cis*-[(en)PtCl(UH-*N*1)] (**1**). Upon hydrolysis of the chloride ligand, the monomeric complex spontaneously tetramerises to the cyclic complex $[(en)Pt(\mu\text{-UH-}N1,N3)]_4^{4+}$ (**2**) [15]. **2** crystallises (as NO_3^- salt) in a 1,3-alternate arrangement, meaning that oppositely positioned uracil bases adopt pairwise identical orientations, viz. have their *O*2 groups up and down, respectively. This conformation is strongly stabilised by the formation of short $O2H\cdots O4$ H-bonding interactions between adjacent uracil heterocycles (Fig. 3).

The resemblance of this compound with purely organic calix[4]arenes [16] is obvious and, consequently, it was termed "*metallacalix*[4]*arene*". In this calix[4]arene analogue, the phenol and methylene groups have been replaced by the uracil and ethylenediamineplatinum(II) moieties, respectively. As in the calix[4]arenes, the partially hindered rotation of the pyrimidine nucleobases about the Pt–N bonds, permits conformational changes in solution. In the case of **2**, this equilibrium is pH dependent and influenced by the presence of additional transition metal ions. Indeed, the conformers of cation **2** have been proven to be unique in the sense that they can act as both cation binders (due to the availability of exocyclic oxygen donors in 2- and 4-positions in the alternate conformer [17] or to the 2-positions in the case of the cone conformer [18]) and as anion receptors inside the hydrophobic cavity of the cone conformer, both in the solid state and in solution [18]. As an example, Fig. 4. shows the formation of a helix of $[(en)_4Pt_4(\mu_4\text{-U-}N1,N3,O2,O4)_4Zn(H_2O)_2]_n^{2n+}$ formula (**3**) with the **2** residues exhibiting a cone conformation strongly stabilised after $[Zn(H_2O)_2]^{2+}$ binding at their oxo-surface. The charge of this system is partially balanced by $Tol\text{–}SO_3^-$ counterions with their hydrophobic residues pointing inside the metallacalix[4]arene cavities.

2.1.2. Hydroxypyrimidine metallacalix[n]arenes

An even closer structural resemblance to calixarenes can be achieved by employing 2-hydroxypyrimidine instead of uracil in $[(en)M(2\text{-pymo-}N1,N3)]_4^{4+}$ ($M = Pd^{II}$

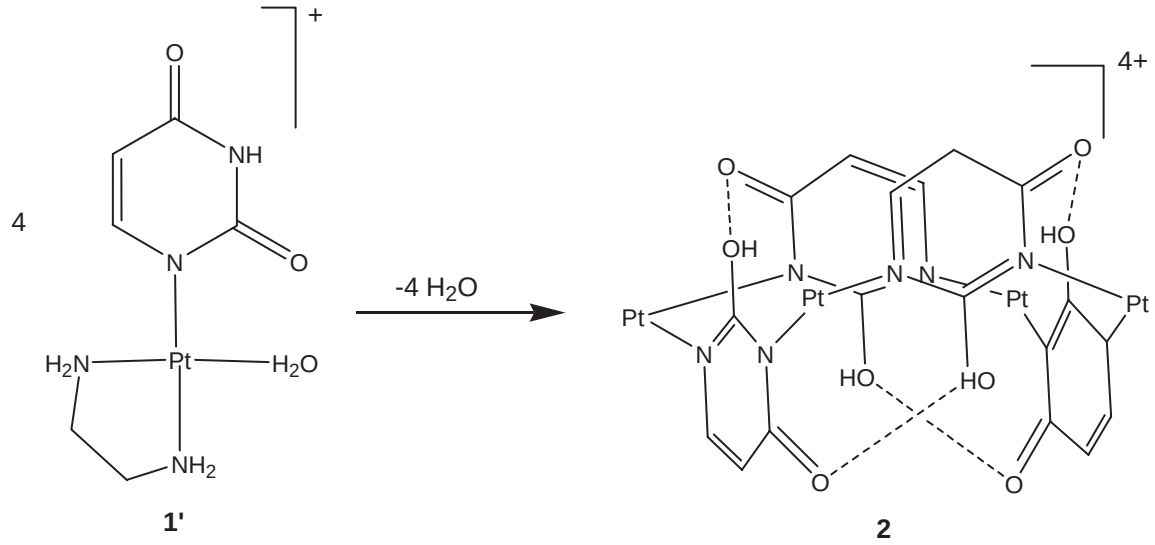

Fig. 3. Self-assembly of $[(en)Pt(H_2O)(UH\text{-}N1)]^+$ (**1′**) to the calix[4]arene analogue $[(en)Pt(\mu\text{-}UH\text{-}N1,N3)]_4^{4+}$ (**2**) in its 1,3 alternate conformation [15].

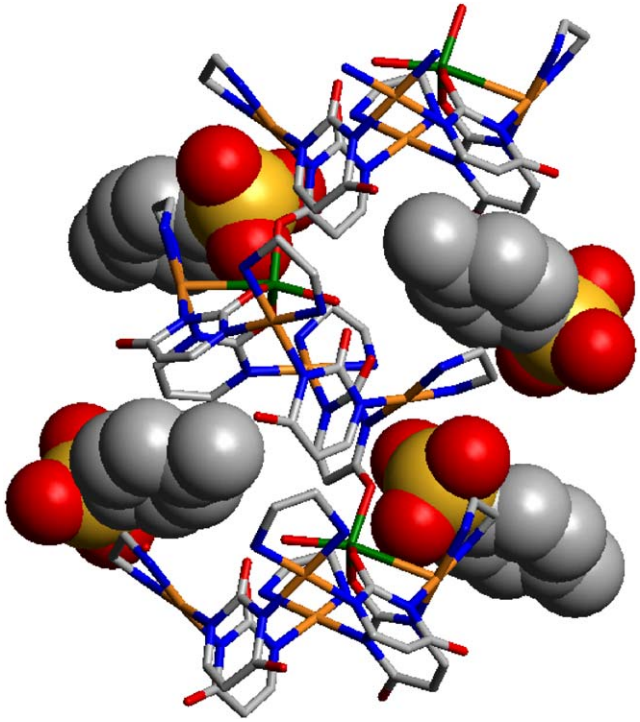

Fig. 4. $[(en)_4Pt_4(U\text{-}N1,N3,O2,O4)_4Zn(H_2O)_2]_n^{2n+}$(**3**) helix and Tol–$SO_3^-$ counterions (Zn; Pt; S; C; N; O). This result shows the ability of the $[(en)_4Pt_4(U\text{-}N1,N3)_4]$ (**2**) species as an ion pair receptor. The insertion of the hydrophobic residues of the sulfonate anions in the cone cavities should be noted [18].

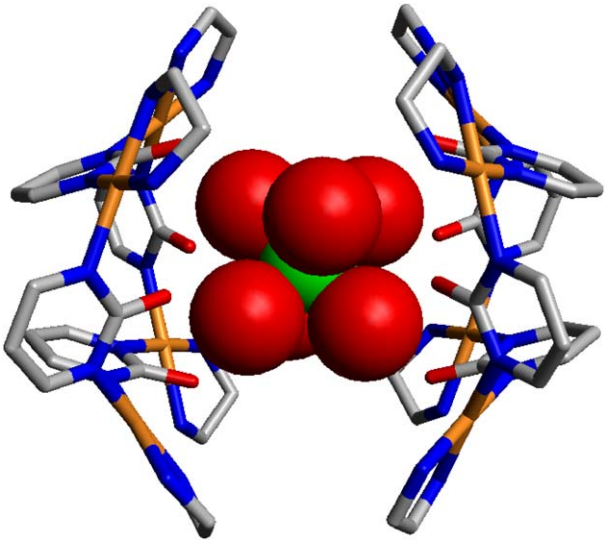

Fig. 5. View of the supramolecular association $\{([(en)Pt(2\text{-}pymo\text{-}N1,N3)]_4)_2[Cu(H_2O)_6]\}^{10+}$ resulting from the molecular recognition of $[Cu(H_2O)_6]^{2+}$ ions by the $[(en)Pt(2\text{-}pymo\text{-}N1,N3)]_4^{4+}$ (**5**) oxo-surface (Pt, Cu, C, N, O) [19].

(**4**) and Pt^{II} (**5**)) systems. The lack of an oxygen in the 4 position results in an almost free rotation about the *M*–N bonds leading to highly conformationally flexible metallacalixarenes. The X-ray crystallographic studies on the nitrate salts of species **4** and **5** show a 1,3-alternate conformation. However, cocrystallisation of **5** with $[Cu(H_2O)_6]^{2+}$ results in two $[(en)Pt(2\text{-}pymo\text{-}N1,N3)]_4^{4+}$ (**5**) moieties sandwiching a $[Cu(H_2O)_6]^{2+}$ ion between their oxo surfaces, which adopt a pinched-cone conformation to give the supramolecular $[\{[(en)Pt(2\text{-}pymo\text{-}N1,N3)]_4\}_2[Cu(H_2O)_6]]^{10+}$ system (Fig. 5) [19]. This result also points to a more reduced basicity of the exocyclic oxygen atoms in **4** and **5** species compared to **2**, which apparently prevents direct coordination of other metal ions to the oxo surface. Indeed, titration of **5** with $HClO_4$ does not lead to calix protonation but to

isolation of a $H_{20}O_8^{4+}$ protonated water cluster encapsulated by two **5** cations [19].

On the contrary, by reacting 4,6-dimethyl-2-hydroxypyrimidine and [(en)Pd^{II}] and cocrystallising the resulting metallacalix[4]arene with the hard Gd^{3+} metal ion resulted in the formation of the capped metallacalixarene $[(en)_4Pd_4(2\text{-dmpymo-}N1,N3,O2)_4Gd(NO_3)_2(H_2O)]^{5+}$ (**6**), which could be fully characterised by X-ray diffraction, showing the simultaneous coordination of the four exocyclic *O*2 atoms to Gd^{3+} (Fig. 6) [20]. The direct interaction of Gd with the metallacalixarene oxosurface is also responsible for the cone conformation fixation, which is the most appropriate for giving host–guest interactions.

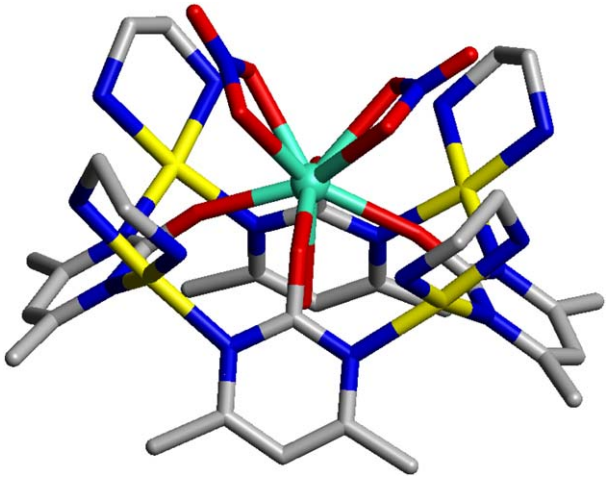

Fig. 6. Structure of $[(en)_4Pd_4(2\text{-dmpymo-}N1,N3,O2)_4Gd(NO_3)_2(H_2O)]^{5+}$ (**6**) (Gd, Pd, C, N, O) [20].

2.1.3. Homochiral metallacalixarenes. Enantioselective recognition of AMP

Enantiopure metallacalix[*n*]arenes can also be synthesised by employing pure *R*,*R*-1,2-diaminecyclohexane (*R*,*R*-dach) or *S*,*S*-1,2-diaminecyclohexane (*S*,*S*-dach), instead of ethylenediamine, as *cis* blocking ligand [21].

The most stable species are the tetranuclear metallacalix[4]arenes, which could be obtained in all cases. However, a hexanuclear species, namely $[(dach)Pd(2\text{-dmpymo-}N1,N3)]_6^{6+}$ (**7**), has also been isolated and fully characterised. The ^1H NMR experiments show, upon heating, a slow conversion process of $[(dach)Pd(2\text{-dmpymo-}N1,N3)]_6^{6+}$ (**7**) into the thermodynamically stable species $[(dach)Pd(2\text{-dmpymo-}N1,N3)]_4^{4+}$ (**8**) (Fig. 7).

The receptor properties of these metallacalixarenes towards mononucleotides have been explored. The results show that an enantioselective recognition process between $[(R,R\text{-dach})Pd(2\text{-dmpymo})]_4^{4+}$ (**8a**) and $[(S,S\text{-dach})Pd(2\text{-dmpymo})]_4^{4+}$ (**8b**) towards AMP takes place in aqueous media (Fig. 8).

2.2. Metallacalixarenes containing 4,7-phenanthroline bridges

2.2.1. Homotopic metallacalixarenes

The versatile host–guest properties of pyrimidine metallacalixarenes prompted us to study related systems. Yu et al. [22] have recently reported the formation of conformationally rigid metallacalix[3]arenes of $[(en)M(4,7\text{-phen})]_3^{6+}$ type, with $M = Pd$ (**9**) and Pt (**10**). We have prepared the homochiral species $[(R,R\text{-dach})Pd(4,7\text{-phen})]_3^{6+}$ (**11a**) and $[(S,S\text{-dach})Pd(4,7\text{-phen})]_3^{6+}$ (**11b**) and studied the receptor properties of **9** and **11** towards mononucleotides (Fig. 9). The results show that

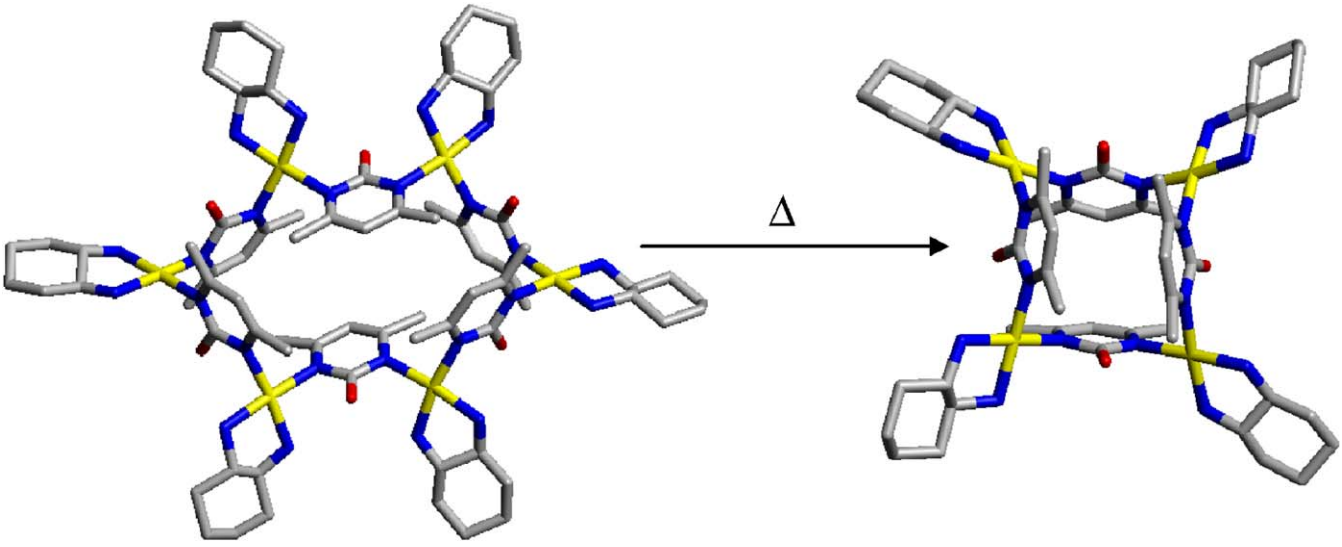

Fig. 7. Conversion of the metallacalix[6]arene $[(dach)Pd(2\text{-dmpymo})]_6^{6+}$ (**7**) into the thermodynamically favoured $[(dach)Pd(2\text{-dmpymo})]_4^{4+}$ (**8**) metallacalix[4]arene upon heating at 60 °C for 6 h. Coordinates from crystal structures of the nitrate salts of **7** and **8** (Pd; C; N; O) [21].

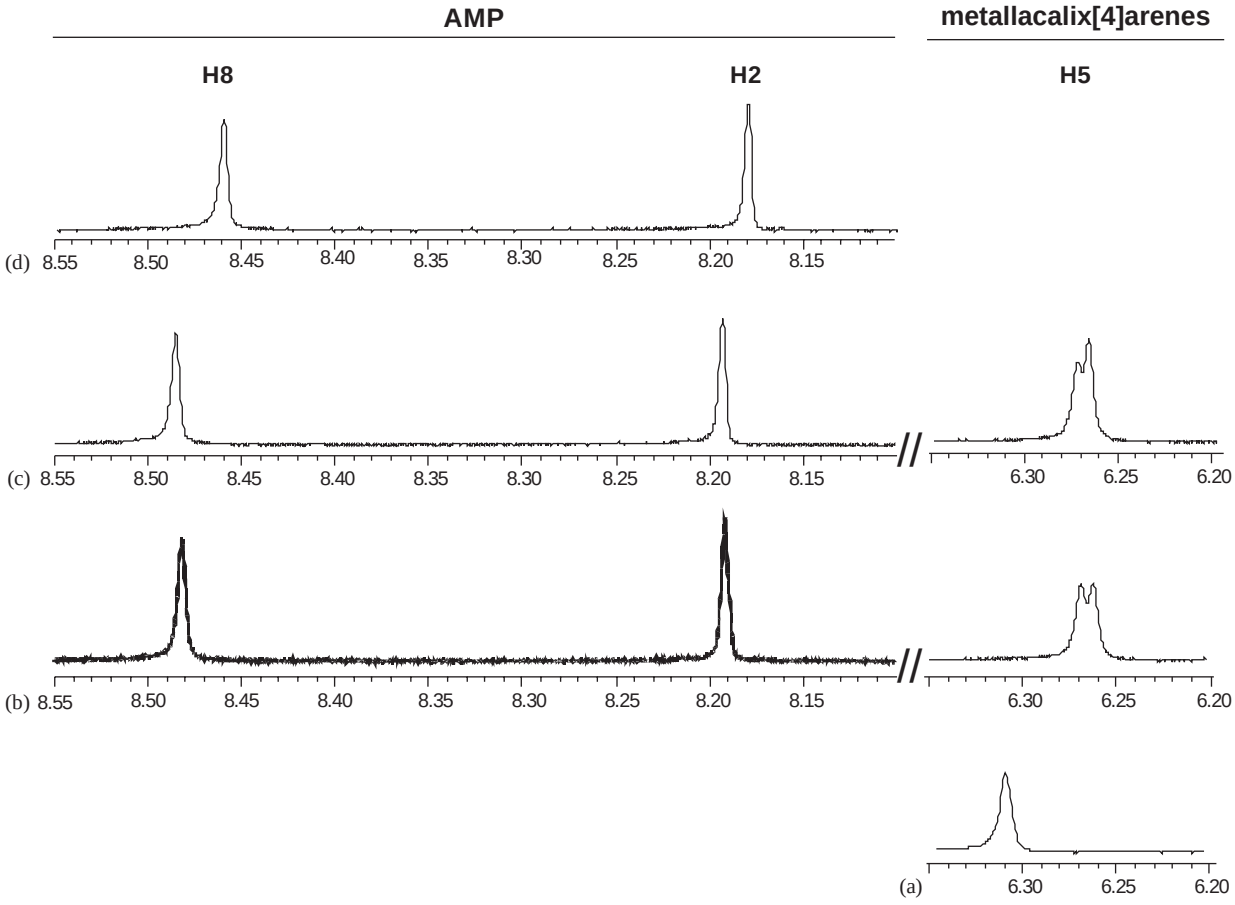

Fig. 8. (a) H5 signal corresponding to a solution containing, simultaneously, $[(R,R\text{-dach})Pd(2\text{-dmpymo})]_4(NO_3)_4$ (**8a**) and $[(S,S\text{-dach})Pd(2\text{-dmpymo})]_4(NO_3)_4$ (**8b**) enantiomers (1:1 ratio). (b) Splitting of the metallacalix[4]arene H5 signal due to the addition of AMP (1:4 ratio). (c) Addition of a larger quantity of the *R,R*-isomer permits unequivocal assignment of the two diasteroisomers. (d) H8 and H2 resonances for free AMP (pH* 6) [21].

both **9** and **11** undertake stronger interactions with mononucleotides than the pyrimidine metallacalixarenes reported before [23]. This recognition process is however followed by metallacalixarene decomposition after ligand displacement by the corresponding mononucleotide.

2.2.2. *Heterotopic metallacalixarenes containing pyrimidine and 4,7-phenanthroline bridges*

The size and shape of metallacalixarene cavities can be modulated by the simultaneous combination of pyrimidine and 4,7-phenanthroline bridges: $[(en)_nPd_n(2\text{-pymo-}N1,N3)_m(4,7\text{-phen-}N4,N7)_{n-m}]^{(2n-m)+}$ [$n=3$, $m=1$ (**12**); $n=4$, $m=2$ (**13**); $n=6$, $m=4$ (**14**)] [24]. These species can be obtained by different reaction pathways, including: (i) reaction of ethylenediaminepalladium(II), 2-pymo and 4,7-phen building blocks and (ii) reaction of the homotopic species $[(en)_4Pd_4(2\text{-pymo-}N1,N3)_4]^{4+}$ (**4**) and $[(en)Pd(4,7\text{-phen-}N4,N7)]_3^{6+}$ (**9**). The resulting heterotopic metallamacrocycles have been characterised by 1D and 2D ^{1}H NMR spectroscopy. Additionally, species **12** and **13** have been studied by X-ray crystallography (Fig. 10). The former contains an almost isosceles triangle of $[(en)_3Pd_3(2\text{-dmpymo-}N1,N3)(4,7\text{-phen-}N4,N7)_2]^{5+}$ formulation, exhibiting a pinched-cone conformation. **13** contains a tetranuclear

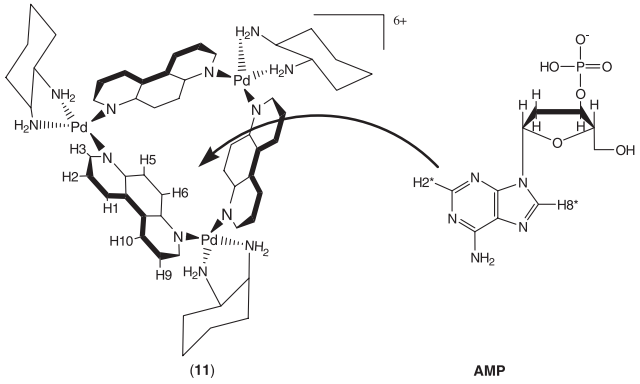

Fig. 9. Mononucleotide recognition process of species **11** towards AMP [23].

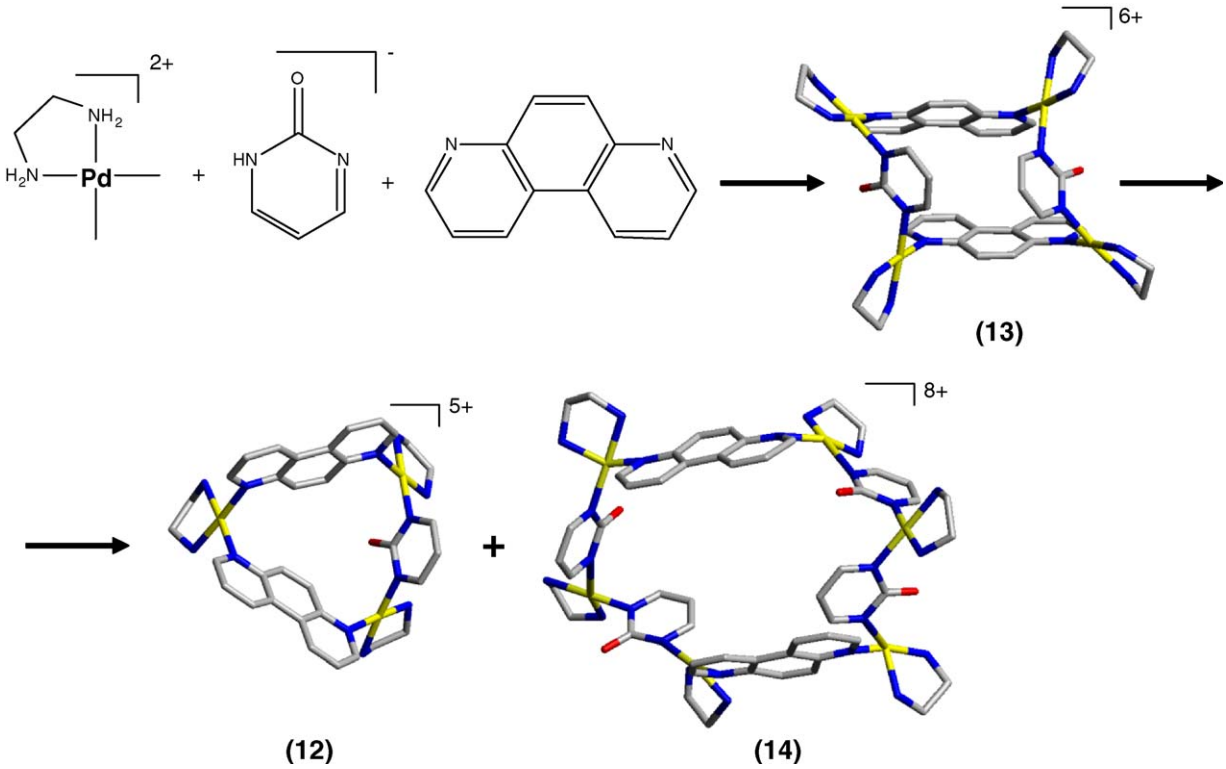

Fig. 10. Reaction of $[(en)Pd(NO_3)^2]$, 2-Hpymo and 4,7-phen building blocks to obtain **13** and posterior disproportionation to **12** and **14**. The coordinates of species **12** and **13** have been taken from the crystal structure of their nitrate salts (Pd, C, N, O) [24].

parallelogram $[(en)_4Pd_4(2\text{-dmpymo-}N1,N3)_2(4,7\text{-phen-}N4,N7)_2]^{6+}$, exhibiting a 1,3-alternate conformation. The host–guest properties of these systems towards mononucleotides have also been studied and showed slightly weaker interactions than **9**, which is related to the smaller opening of their cavities.

3. 1D polymers and hexagons applying linear metal fragments

Combination of linear metal entities with the 120° bond angles provided by the endocyclic N atoms of pyrimidines is compatible with the formation of zig-zag chains, meanders, helixes as well as discrete hexagons (Fig. 1). Although the formation of the latter architecture is entropically favoured over polymeric products [1b], the complexity of the assembly process increases with the number of ring members, implying a considerable degree of rotational freedom in the intermediate structures, which prevents the straightforward isolation of hexagons in most cases. Thus, we have observed the preferential formation of polymeric structures over discrete ones under mild reaction conditions in systems containing linear metal fragments.

In the case of labile Cu^{II} metal ion in combination with 2-Hdmpymo in aqueous amine solutions, we have only observed the formation of the infinite zig-zag 1D polymer *trans*-$[(amine)_2Cu(2\text{-dmpymo-}N1,N3)]_n^{n+}$ (**15**) [25]. Aoyama and coworkers observed a higher versatility in the *M*/pyrimidine system ($M = Co^{II}$, Cu^{II}, Cd^{II}) for the generation of different 1D polymers and helixes as a consequence of metal plasticity [26].

Ag^{I} and 2-Hpymo in an aqueous amine solution lead to the formation of the neutral 1D zig-zag polymeric material $[Ag(2\text{-pymo-}N1,N3)]_n$ (**16**), which has been characterised by conventional X-ray diffraction methods [27]. Thermal treatment of **16** and study of the X-ray powder diffraction patterns shows the sequential formation of an amorphous material, which recrystallises above 150 °C leading to a novel crystalline phase containing the thermodynamically more stable $[Ag(2\text{-pymo-}N1,N3)]_6$ (**17**) hexamers (Fig. 11) [28]. This transformation can also be achieved at r.t. by suspending **16** in ethylorthoformiate for 12 h under stirring.

Similarly, we have also reported the formation of a yellow polycrystalline material by reaction of $[Cu(MeCN)_4]BF_4$ with 2-Hpymo. The ab initio XRPD study has permitted to unravel its complex nature, in which molecular $[Cu(2\text{-pymo-}N1,N3)]_6$ hexagons (**18**) are recognised in the grooves of the polymeric $[Cu(2\text{-pymo-}N1,N3)]_n$ helixes (**19**) (Fig. 12) [29]. This result also proves the low-energy barrier between these two different products. Although the individual helixes

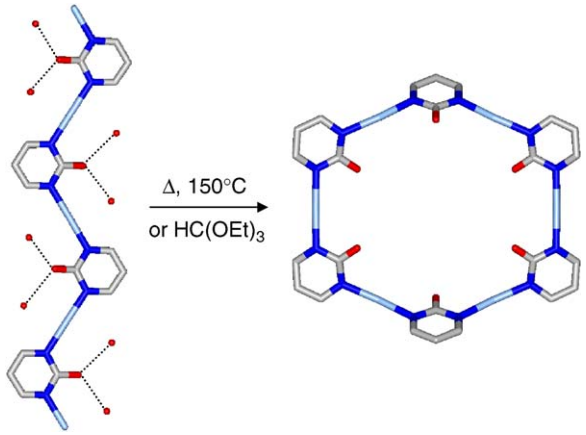

Fig. 11. Conversion of polymeric $[Ag(2\text{-pymo-}N1,N3)]_n$ (**16**) into the thermodynamically favoured hexanuclear $[Ag(2\text{-pymo-}N1,N3)]_6$ (**17**) species (Ag, C, N, O) [28].

are (obviously) chiral, this compound contains helixes of opposite handedness, giving centric crystals. However, we have recently reported that it is possible to obtain acentric SHG active crystals IF 2-nitropymo is employed, affording $[Ag(2\text{-nitropymo-}N1,N3)]_n$ (**20**) helixes [30]. The non linear optical properties of the Ag/5-nitro-2-hydroxypyrimidine system are likely due to the high hyperporalisability of the functionalised pyrimidine which is among the largest for 1,4-disubstituted arenes [31]. In contrast to the examples cited above, in this case the formation of cyclic systems has not been observed.

When slow reaction kinetics metals, i.e. Pt^{II} are used, the formation of supramolecular entities, in a sequential manner, is possible. We have employed the inert *trans*-$[(NH_2R)_2Pt(2\text{-Hpymo-}N1)_2]^{2+}$ (**21**) building block ($R = H$) in combination with the labile Ag^I metal ion to build the heteronuclear 1D polymeric system {*trans*-$(NH_3)_2Pt(2\text{-pymo-}N1,N3)_2Ag]_n^{n+}$ (**22**) (Fig. 13) [32]. It should be noted that its novel meander topology is an additional proof of the high conformational degree of freedom of these materials during their self-assembly process.

Combination of the coordinative bond with the H-bonding possibilities of the organic residues in **21** with other complementary systems is likewise possible. Thus, cocrystallisation of **21** ($R = Me$) with 2-aminopyrimidine (2-ampym) results in the formation of the H-bonding supported supramolecular hexagon *trans*-$[(MeNH_2)_2Pt(2\text{-pymo-}N1)(2\text{-Hpymo-}N1)\cdot 2\text{-Hampym}]_2^{4+}$ (**23**) (Fig. 14) [32]. The resulting supramolecular assembly reveals that its formation is associated with a proton transfer from one of the 2-Hpymo residues to one of the endocyclic N atoms of 2-ampym against a pK_a gradient of 1.5 units. The consequent loss of the original symmetry of both residues (2-ampym and the two 2-Hpymo) due to this proton transfer is apparently favoured by a more even distribution of the positive charge along the supramolecular assembly and a more efficient H-bonding pattern, i.e. instead of two pairs of DA: AD hydrogen bonds, a pair of the more favoured DD:AA scheme is generated [33].

4. Functional 2D and 3D coordination polymers containing metal fragments of higher coordination numbers

4.1. Robust frameworks containing metal ions and hydroxypyrimidines

In the recent past, we have prepared a large number of metal(II) diazolates, such as Zn, Cd, Hg, Co or Ni pyrazolates [34] and Cd, Hg, Cu or Ni imidazolates [35]. All these species have invariably shown polymeric structures, ranging from 1D chains of collinear metal atoms, to 2D frameworks (of square meshes or more complex architectures) up to 3D polymers with, or without, large pores or cavities. Typically, the metal ions are tetracoordinated by diazolate ligands acting in the *N*,*N*′-*exo*bidentate fashion, this leading to crystalline coordination polymers lacking counterions in the lattice and possessing unusually high thermal stability (up to 440 °C for the zinc bispyrazolate species [34a]). Worthy of note, a few case structures have been found, such as the copper bisimidazolate system [35b], in which *five* polymorphic phases were identified (and selectively prepared), and the cadmium and mercury analogues [35a], based upon tightly interpenetrated diamondoid networks.

After having studied the oligonuclear metal complexes reported above, we have turned our attention to the synthesis of $M(X\text{-pymo})_2$ complexes ($X = 2, 4$) with the 2-Hpymo and 4-Hpymo ligands. Through the occasional intermediacy of hydrated species (which can be easily transformed into the homoleptic polymers by controlled heating, water removal and solid–solid phase-transformation), 3D frameworks of the diamondoid-type $[M(2\text{-pymo-}N1,N3)_2]_n$ ($M = Co$ (**24**), Ni (**25**), Zn (**26**)) were initially obtained [36]. In these coordination polymers, the organic moieties bridge (in the common *N*1,*N*3-exobidentate mode) metal centres surrounded by four nitrogen atoms of four different ligands. Only for the nickel derivative, thanks to the higher stability of the octahedral vs. tetrahedral geometry, ancillary Ni–*O*2 bonds are present, thus lowering the crystal symmetry, but maintaining the overall network topology. These species can be defined as thermally robust coordination polymers, the zinc derivative decomposing, under nitrogen, only above 570 °C. Their acentric nature was confirmed by second harmonic generation measurements (Kurtz–Perry method [37]), their SHG efficiency, although measurable, falling below that of standard

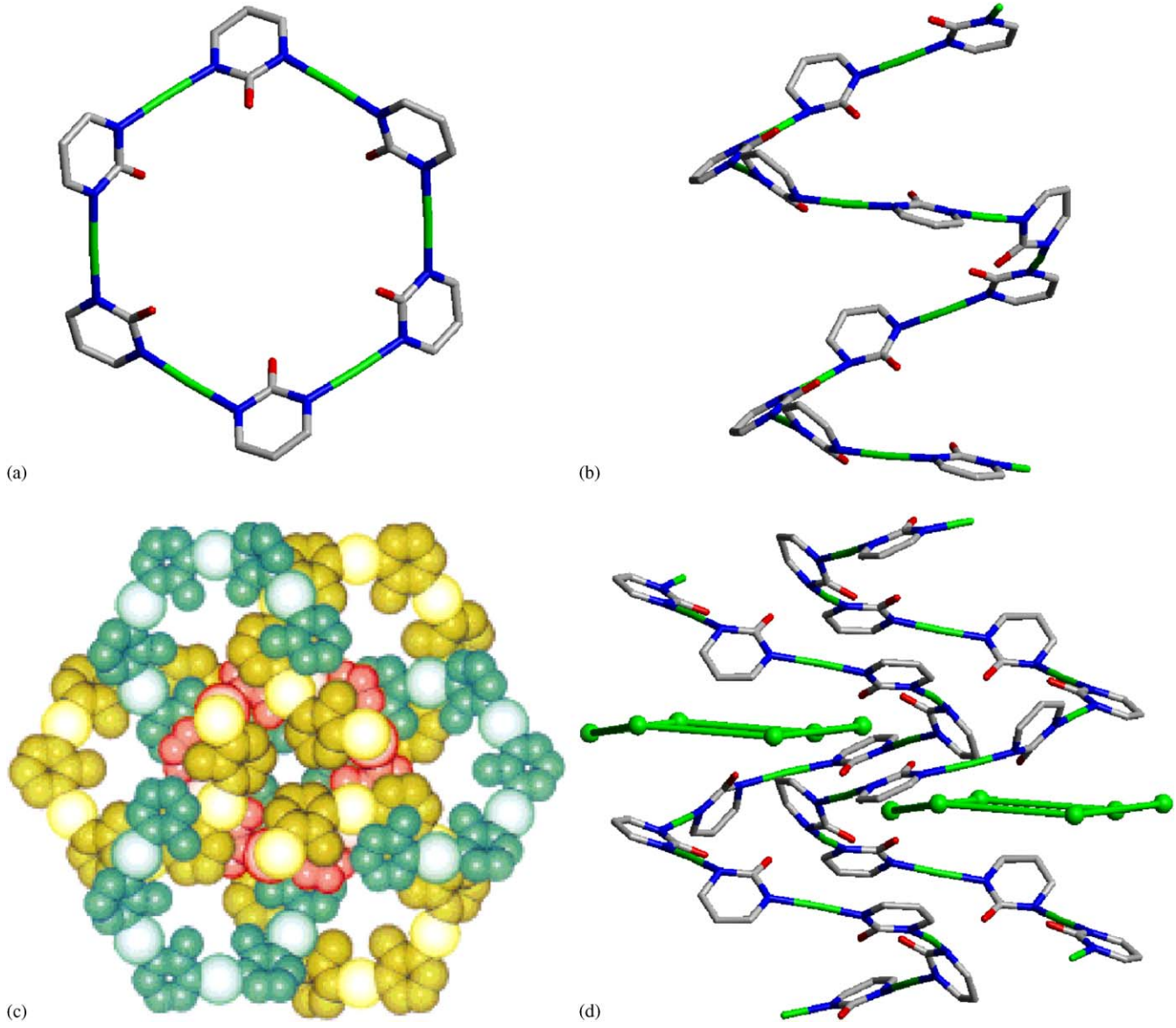

Fig. 12. Crystal structure of the complex phase in which cyclic $[Cu(2\text{-pymo})]_6$ (**18**) hexamers (a) and $[Cu(2\text{-pymo})]_n$ (**19**) helixes (b) (Cu, C, N, O) coexist. (c) Space filling diagram down the crystallographic *c* axis. The helixes of different handedness are shown in different colours (green and yellow) whereas the hexameric guests are shown in red. (d) Schematic view of two helixes of different handedness and hexameric guests hosted in the helixes grooves [29].

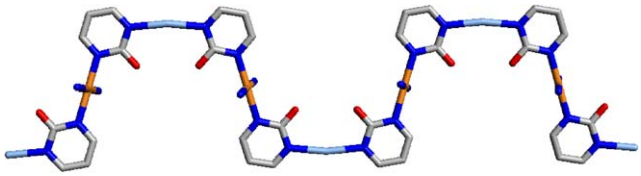

Fig. 13. Crystal structure of the nitrate salt of $\{trans\text{-}(NH_3)_2Pt(2\text{-pymo-}N1,N3)_2Ag\}_n^{n+}$ (**22**) (Pt, Ag, C, N, O) [32].

urea. Moreover, among these coordination polymers, that possessing the most interesting functional properties is $[Co(2\text{-pymo-}N1,N3)_2]_n$ (**24**), which, at temperatures below 23 K, magnetically orders and becomes a molecular magnet [38].

On employing the 4-Hpymo ligand, (hydrogen-bonded) hydrated *mononuclear* species $[M(4\text{-pymo-}N1)_2(H_2O)_4]$ ($M = Co$ (**27**), Ni (**28**)) were obtained, which could be easily transformed into polycrystalline coordination polymers by moderate heating. The obtained $[M(4\text{-pymo-}N1,N3)_2]_n$ ($M = Co$ (**29**) [38], Ni (**30**) [39]) species are markedly different from the 2-pymo analogues: indeed, the basic topology is based upon 2D sheets of square meshes, where the metals are bridged by 4-pymo ligands in the uncommon *N*1,*O*4 mode (with an ancillary long interaction by the *N*3 atom). The metals

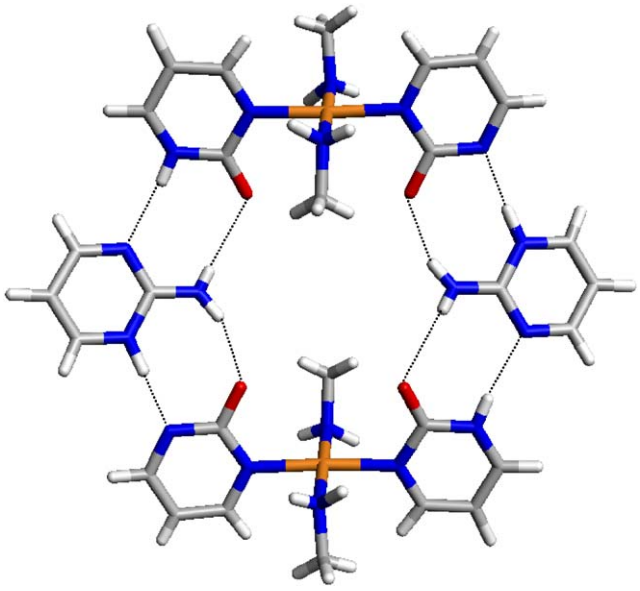

Fig. 14. Crystal structure of the supramolecular hexagon *trans*-$[(MeNH_2)_2Pt(2\text{-pymo-}N1)(2\text{-Hpymo-}N1)\cdot 2\text{-Hampym}]_2^{4+}$ (**23**). The presence of two different H-bonding schemes DA:AD and DD:AA at either side of the 2-ampym moieties arises from a proton transfer against a pK_a gradient from **22** to ampym (Pt, C, N, O) [32].

are therefore hexacoordinated, in a distorted octahedron of C_{2v} symmetry. At variance, no hydrated precursor was observed for [Zn(4-pymo-*N*1,*N*3)(4-pymo-*N*1,*O*4)]$_n$ (**31**) [39] and an unprecedented three-dimensional network built upon tetrahedral nodes and 4-pymo bridges of the *N*1,*N3* and *N*1,*O*4 type was observed ($6_26_26_28_26_36_3$; $C_{10} = 426$) [40].

More recently, we decided to explore the coordination chemistry of the extremely polarised heterocycle 5-nitro-2-hydroxypyrimidine, aiming to improve the SHG efficiency of these materials adding this function to other desirable properties. We initially studied the [Co(2-nitropymo-*N*1,*N*3)(2-nitropymo-*N*1,*O*2)]$_n$ (**32**), [Ni(2-nitropymo)$_2$]$_n$ (**33**) and [Zn(2-nitropymo-*N*1,*N*3)(2-nitropymo-*N*1,*O*2)$_2$]$_n$ (**34**) polymers [41], which (owing to the centrosymmetric nature of their structures) afforded inactive SHG species, thus vanishing our first efforts. However, these materials showed interesting magnetic properties and, for the two polycrystalline species (**32**,**34**), less common N_3O chromophores. Our latest studies, performed on using Ag(I) ions (as discussed above and in Ref. [30]), indicated the formation of acentric SHG active materials, prompting for a more extensive characterisation of other metal organic frameworks based on this ligand.

4.2. Open metal organic frameworks containing metal ions and hydroxypyrimidines

In all the 2D and 3D species presented above, the metals were either tetrahedral or, more rarely, (pseudo)octahedral. At variance, square-planar metal centres have been found in the [Cu(*X*-pymo-*N*1,*N*3)$_2$]$_n$ ($X = 2$ (**35**) [42], 4 (**36**) [43]) species, with open sodalitic frameworks built upon four- and six-membered rings (metalla[4]- and metalla[6]calixarenes and planar molecular hexagons) hinged about the Cu(II) ions (Fig. 15).

These species are easily formed by self-assembling processes, and typically host water or other solvents as well as ions in the large cavities of such their nanoporous framework. In order to probe their functionality, they were submitted to gas sorption and ion pair recognition processes. The histeresis loops found in the solid-liquid ion pair sorption isotherms were indicative of reversible guest-induced phase transitions (Fig. 16).

The observed guest-induced phase transitions found in **35** and **36** systems were extensively studied by X-ray powder diffraction methods. These species were submitted to heating cycles (testing the reversibility of the hydration/dehydration process) and to exposure to solutions of simple salts in different solvents. The large number of observations gathered in the last years in our laboratories can be summarised as follows, the important structural changes characterised by diffraction methods being illustrated in Fig. 17:

(a) [Cu(2-pymo-*N*1,*N*3)$_2$]$_n$ (**35$_R$**), in its hydrated form, contains ca. 2.5 water molecules per Cu(II) ion and the sodalitic framework possesses a pseudocubic

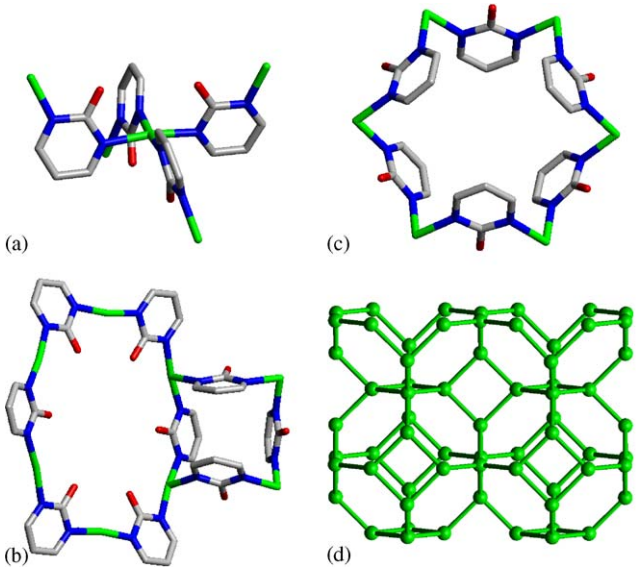

Fig. 15. (a) Coordination about the copper centres in [Cu(2-pymo-*N*1,*N*3)$_2$]$_n$ (**35**). (b,c) Planar hexagons, metallacalix[4]arenes and metallacalix[6]arenes basic structural motives interlock to build a highly symmetric 3D sodalitic framework (d). The green balls and rods represents Cu centres and 2-pymo bridges, respectively (Cu, C, N, O).

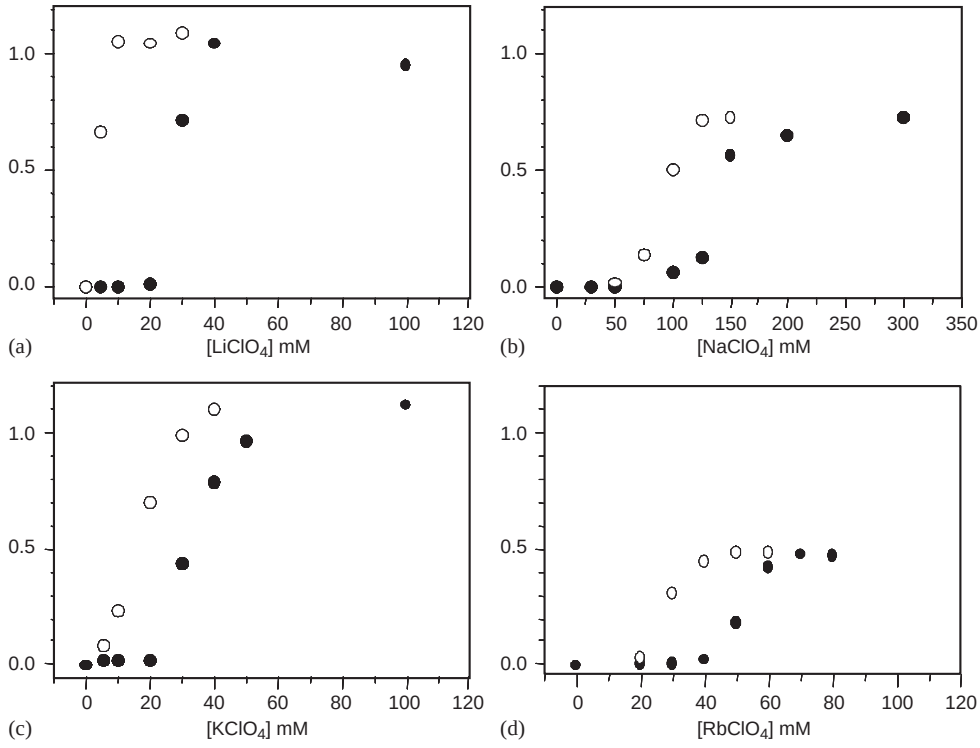

Fig. 16. Sorption isotherms data at 298 K for **35** with group 1 metal perchlorate salts. $LiClO_4$ (a); $NaClO_4$ (b); $KClO_4$ (c); $RbClO_4$ (d). Open symbols indicate desorption. It should be noted that in the $RbClO_4$ case only partial occupancy is achieved which might be due to Rb^+ higher size. The observed hysteresis loops are indicative of a guest induced phase transition [42a].

R-3m lattice, with two Cu(II) ions slightly differentiated by distinct $Cu \cdot OH_2$ interactions.

(b) Upon gentle heating, above 60 °C, water molecules are lost and a truly cubic, evacuated, Pn-3m structure (**35$_C$**) is formed (Fig. 18). This species restores the original trigonal one if cooled down to r.t. in moist air. The process, although reversible, shows a remarkable hysteretic effect.

(c) If crystallised in the presence of alkali metal (and ammonium) *MX* salts of 'cubic' anions (such as BF_4^-, ClO_4^- and PF_6^-), these ion pairs are 'recognised' by the planar hexagonal windows, and highly crystalline species $[Cu(2\text{-pymo-}N1,N3)_2 \cdot (MX)_{1/3}]_n$ (**35$_C$@MX**), containing stoichiometric amounts of the salts, are obtained (Fig. 19a) [42a].

(d) Using different solvent mixtures and/or anions, inclusion is still observed, but, when large cations are employed, an irreversible guest-induced phase transformation to an orthorhombic laminar phase $[Cu(2\text{-pymo-}N1,N3)_2 \cdot (MX)_{1/2}]_n$ (**35$_O$@MX**), is observed, where only metalla[4]calixarene windows in cone conformation are found; in this type of structure, four neighbouring oxygen atoms typically bind the large cations on one side, leaving space for nitrate (and water) *M–O2* bonds on the opposite face (Fig. 19b) [42b].

(e) Removal of the guests intercalated in these 'muscovitic' laminae can be achieved by suspending the material in crown ether solutions, affording an empty laminar $[Cu(2\text{-pymo-}N1,N3)_2]_n$ (**35$_O$**) species, i.e. a true polymorph of the evacuated sodalitic phase [42b].

(f) At variance, the sodalitic framework $[Cu(4\text{-pymo-}N1,N3)_2]_n$ (**36**), in its (tris)hydrated (r.t.) and evacuated (140 °C) forms is *persistently* cubic, Pn-3m, but shows a progressive shrinking of the unit cell volume upon heating. The hydration/rehydration process is fully reversible [43].

(g) The disposition of the oxygen rings, pointing toward different cavities in the 2-pymo or 4-pymo derivatives, significantly modify the hydro-/lipo-philicity of the tunnels, and is clearly responsible for the different low-temperature N_2 sorption behaviour ($\sim 10x$ less effective in **36** than for the *isomorphous* **35** analogue).

(h) Accordingly, the sorption of ion pairs by **36** is much more limited, and no evidence for stoichiometric species characterised by selective recognition of specific ions and a (more or less) ordered crystal structure was up to now observed.

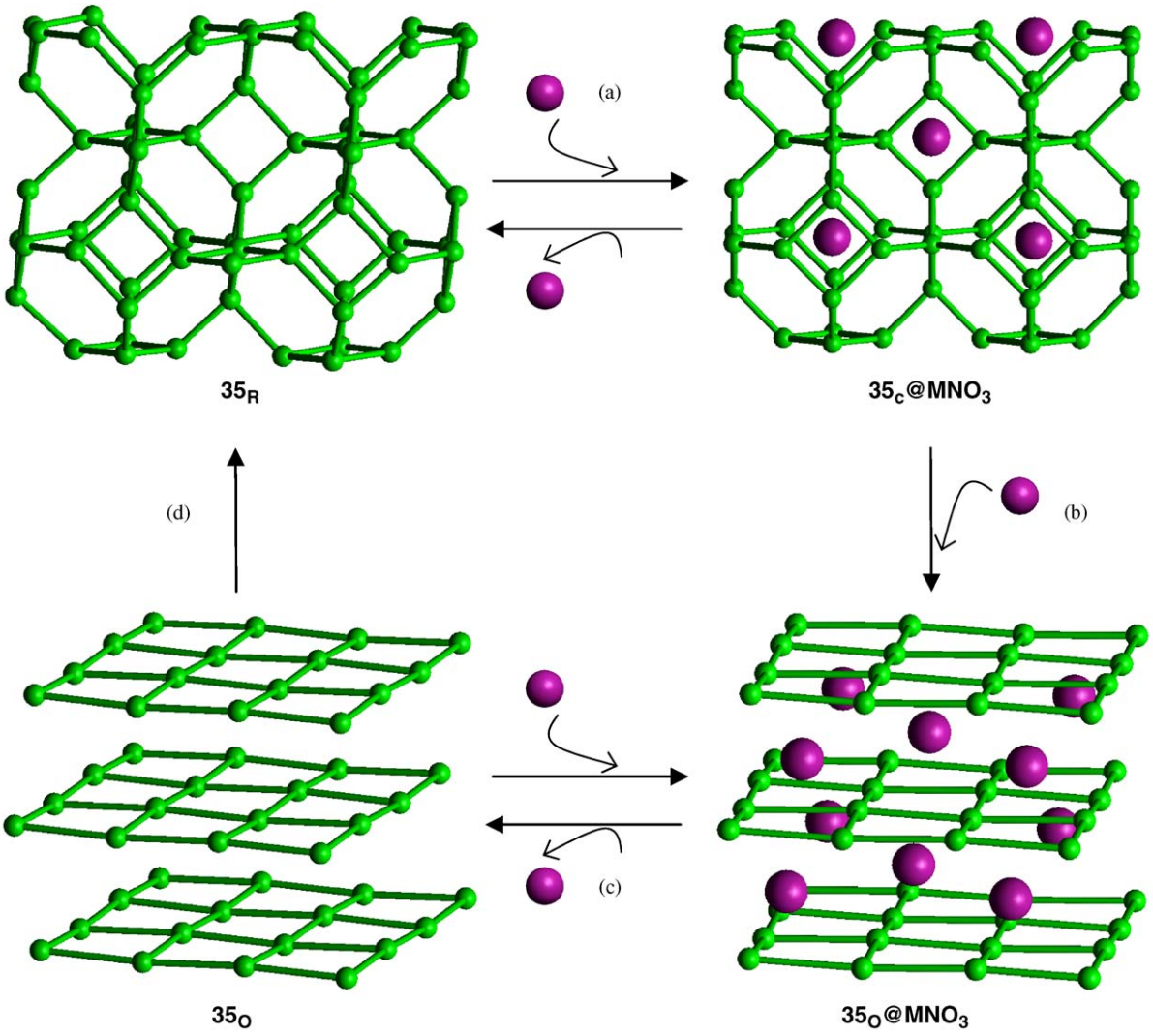

Fig. 17. Guest induced crystal to crystal phase transitions taking place on $[Cu(2\text{-pymo-}N1,N3)_2]_n$ (**35_R**) upon MNO_3 ion pair incorporation from water/methanol solutions. (a) Inclusion of $n/3$ MNO_3; (b) Additional inclusion of $n/6$ MNO_3; (c) removal of $n/2$ MNO_3 guests by treatment with 18-crown-6-ether; (d) Exposition of **35_O** to water. Green balls, green rods and purple balls represent copper centres, 2-pymo bridges and MNO_3 ion pair guests, respectively.

4.3. Mixed ligand layered systems

Formation of mixed ligand extended polymers is also possible. Indeed, we have observed that a one-pot reaction of Cu(II) salts with 2-Hpymo · HCl and 4,4′-bipyridine (4,4′-bpy) leads to the formation of a series of isomorphous extended 2D layered frameworks of $[Cu_3(\mu\text{-OH})_2(\mu\text{-Cl})_2(\mu\text{-2-pymo})(\mu\text{-4,4′-bpy})_3]_nX_n \cdot mH_2O$ type, where $X = NO_3$ (**37a**), Cl (**37b**), ClO_4 (**37c**), AcO (**37d**), $SO_4/2$ (**37e**) (Fig. 20a), which can be related to the family of clay minerals [44]. Although these materials are not able to include N_2 at 77 K, their porous nature has been derived from XRPD studies. A swelling response perpendicular to the layers (along a), concomitant to aliphatic alcohol inclusion in the interlayer voids, is observed (Fig. 20b). This type of observation further strengthens the mineralomimetic behaviour of these materials.

5. Conclusions and perspectives

The bent bond angles provided by the endocyclic N atoms of the pyrimidine moieties lead to more unpredictable architectures compared to classical rod type spacers. For the latter, the rotation about the *M*–N bonds should not play, in principle, an important role in the resulting architecture. This situation contrasts the

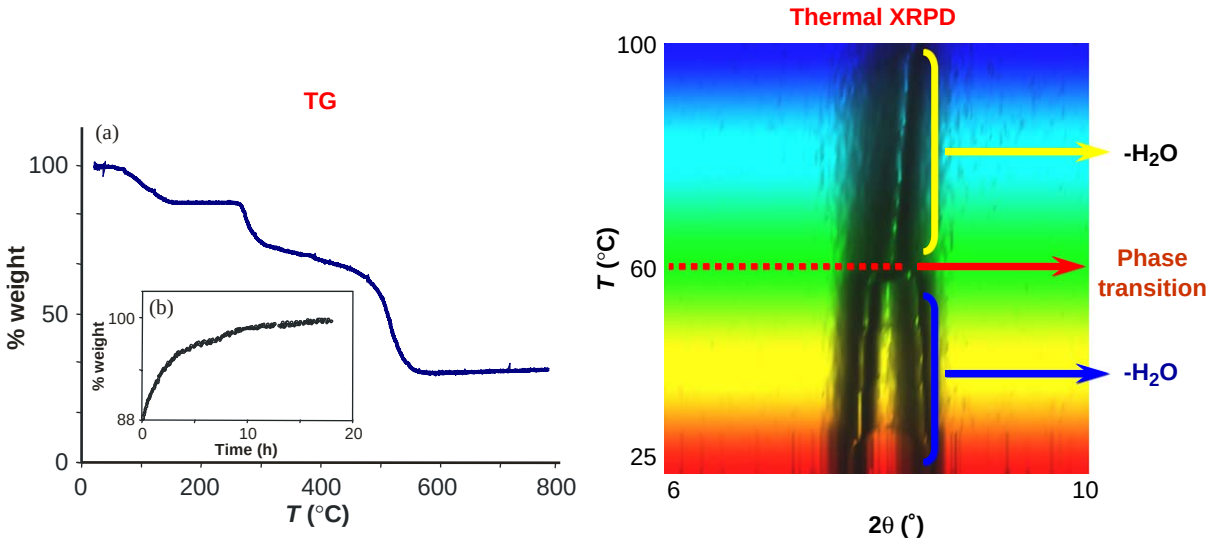

Fig. 18. Thermogravimetric analysis of **35** (left) and rehydration process upon exposition of the evacuated material to moist air (onset on the left) [42a]. Variable temperature XRPD traces in the 6–10° 2θ range (right), showing the progressive merging of the 110 and 012 peaks of the rhombohedral $\mathbf{35_R}$ phase into the 110 reflection of the evacuated cubic $\mathbf{35_C}$ ($a_0 = 15.07$ Å) phase. Vertical scale, T in the 25–100 °C range (bottom to top, 10 scans per 10 °C interval). At each T, equilibrium is fully reached. Coalescence occurs at 60 °C [42b].

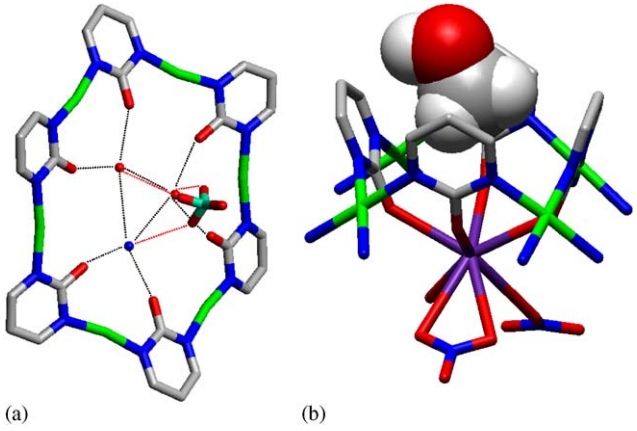

Fig. 19. (a) Supramolecular recognition of $[NH_4 \cdot 2H_2O]ClO_4$ in the hexagonal windows of the sodalite β-cages in $\mathbf{35_C@NH_4ClO_4}$. (b) The metallacalix[4]arene motif in $\mathbf{35_O@RbNO_3}$: the lower rim recognises $RbNO_3(H_2O)$, the cone cavity MeOH. (Cu, Rb, C, N, O) [42].

one found for bent spacers, in which any rotation about the *M*–N bonds will have a dramatic effect on the self-assembly process.

Another interesting feature of this type of bent ligands is that, in spite of their rigid nature, it is possible to obtain flexible frameworks. In contrast to the situation found for plastic materials containing flexible ligands, their plasticity does not arise from the ligands themselves but from the rotation about the *M*–N bonds.

The functionalisation of the pyrimidine moieties leads to functional cavities, pores and surfaces able to interact with additional species through coordinative bonds, H-bonding, electrostatic and hydrophobic interactions.

The mineralomimetic nature of the extended systems should be noted. However, important differences arise in the charge and flexibility of the structural frameworks and in the polarity of the cavities. It should also be noted that the structural motives found in the discrete systems are also present in the extended ones. The same situation is found for the active recognition sites. This feature is very important to unequivocally establish, at the molecular level, the recognition processes and guest induced phase transitions taking place in the extended systems.

The extensive use of XRPD methods has been very useful for the characterisation of many of the extended materials obtained *only* in polycrystalline form, from either conventional synthetic methods or solid-to-solid reactions. Without this technique, many structural details of these species and of the structural transformations taking place on them upon guest incorporation would have remained obscured.

Finally, it should be noted that some of these materials combine also additional interesting magneto-optical properties. Thus, further work can be anticipated in the direction of preparing differently substituted Hpymo ligands, to be coupled with a number of transition metal ions, and to the discovery of multi-functional materials, where optical, magnetic and

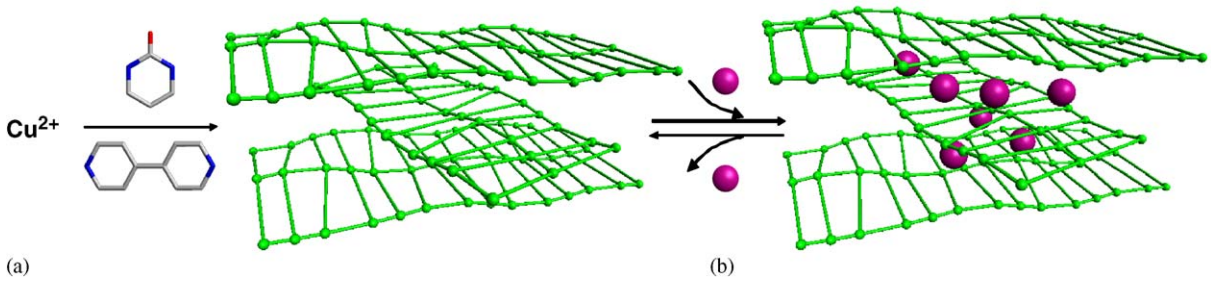

Fig. 20. (a) Synthesis of the **37** isomorphous series. (b) Swelling response to aliphatic alcohols. Cu (green balls), 2-pymo, 4,4′-bpy, Cl and OH bridges (green rods). The purple spheres denote the aliphatic alcohol guests.

nanoporosity properties can be possibly optimised and actively used in applied fields.

References

[1] (a) J.M. Lehn, Supramolecular Chemistry, VCH, Weinheim, 1995;
(b) S. Leininger, B. Olenyuk, P.J. Stang, Chem. Rev. 100 (2000) 853;
(c) M. Fujita, K. Umemoto, M. Yoshizawa, N. Fujita, T. Kusukawa, K. Biradha, Chem. Commun. (2001) 509;
(d) G.F. Swiegers, T.J. Malefetse, Chem. Rev. 100 (2000) 3483;
(e) R.W. Saalfrank, E. Uller, D. Demleitner, I. Bernt, Struct. Bond. (Berlin) (2000) 96;
(f) F. Hof, S.L. Craig, C. Nuckolls, J. Rebek, Angew. Chem. Int. Ed. 41 (2002) 1488.

[2] A.J. Petrella, N.J. Roberts, D.C. Craig, C.L. Raston, R.N. Lamb, Chem. Commun. (2003) 1014.

[3] For numerous applications, see, e.g.: Special issue of *PNAS* (Supramolecular Chemistry and Self-Assembly), 99:8, 2002.

[4] (a) T. Kusukawa, M. Fujita, J. Am. Chem. Soc. 121 (1999) 1397;
(b) M. Yoshizawa, T. Kusukawa, M. Fujita, K. Yamaguchi, J. Am. Chem. Soc. 122 (2000) 6311;
(c) M. Yoshizawa, Y. Takeyama, T. Kusukawa, M. Fujita, Angew. Chem. Int. Ed. 41 (2002) 1347.

[5] (a) K.J. Balkus Jr., Prog. Inorg. Chem. 50 (2001) 217;
(b) X. Bu, P. Feng, G.D. Stucky, Science 278 (1997) 2080.

[6] H. Maas, G. Calzaferri, Angew. Chem. Int. Ed. 41 (2002) 2284.

[7] (a) S. Kitawaga, R. Kitaura, S. Noro, Angew. Chem. Int. Ed. 43 (2004) 2334;
(b) H.K. Chae, D.Y. Siberio-Pérez, J. Kim, Y. Go, M. Eddaoudi, A.J. Matzger, M. O'Keeffe, O.M. Yaghi, Nature 427 (2004) 523;
(c) D.V. Soldatov, J. Inclusion Phenom. 48 (2004) 3;
(d) M.J. Rosseinsky, Micropor. Mesopor. Mater. 73 (2004) 15;
(e) C. Janiak, Dalton Trans. (2003) 2781;
(f) S.L. Stuart, Chem. Soc. Rev. 32 (2003) 276;
(g) S. Kitagawa, S. Masaoka, Coord. Chem. Rev. 246 (2003) 73;
(h) B. Moulton, M.J. Zaworotko, Chem. Rev. 101 (2001) 1629;
(i) O.M. Yaghi, H. Li, C. Davis, D. Richardson, T.L. Groy, Acc. Chem. Res. 31 (1998) 474;
(j) S. Kitagawa, M. Kondo, Bull. Chem. Soc. Jpn. 71 (1998) 1739.

[8] E. Coronado, J.R. Galán-Mascarós, C.J. Gómez-García, V. Laukhin, Nature 408 (2000) 447.

[9] R. Kitaura, G. Onoyama, H. Sakamoto, R. Matsuda, S.-I. Noro, S. Kitagawa, Angew. Chem. Int. Ed. 43 (2004) 2684.

[10] (a) S.J. Lee, W. Lin, J. Am. Chem. Soc. 124 (2002) 4554;
(b) J.S. Seo, D. Whang, H. Lee, S.I. Jun, J. Oh, Y.J. Jeon, K. Kim, Nature 404 (2000) 982.

[11] (a) X. Zhao, B. Xiao, A.J. Fletcher, K.M. Thomas, D. Bradshaw, M.J. Rosseinsky, Science 306 (2004) 1012;
(b) R. Kitaura, K. Seki, G. Akiyama, S. Kitagawa, Angew. Chem. Int. Ed. 43 (2004) 428;
(c) X.H. Bu, M.L. Tong, H.C. Chang, S. Kitagawa, S.R. Batten, Angew. Chem. Int. Ed. 43 (2004) 192;
(d) D.N. Dybtsev, H. Chun, S.H. Yoon, D. Kim, K. Kim, J. Am. Chem. Soc. 126 (2004) 32;
(e) R. Kitaura, K. Seki, G. Akiyama, S. Kitagawa, Angew. Chem. Int. Ed. 42 (2003) 428;
(f) N.L. Rosi, J. Eckert, M. Eddaoui, D.T. Vodak, J. Kim, M. O'Keefe, O.M. Yaghi, Science 300 (2003) 1127;
(g) M. Eddaoudi, J. Kim, N. Rosi, D. Vodak, J. Wachter, M. O'Keefe, O.M. Yaghi, Science 295 (2002) 469.

[12] W. Saenger, Principles of Nucleic Acid Structure, Springer, New York, 1984.

[13] S.W. Keller, Angew. Chem. Int. Ed. 36 (1997) 247.

[14] (a) J.A.R. Navarro, B. Lippert, Coord. Chem. Rev. 185–186 (1999) 653
(b) Coord. Chem. Rev. 222 (2001) 219.

[15] (a) H. Rauter, E.C. Hillgeris, B. Lippert, J. Chem. Soc., Chem. Commun. (1992) 1385;
(b) H. Rauter, E.C. Hillgeris, A. Erxleben, B. Lippert, J. Am. Chem. Soc. 116 (1994) 616.

[16] (a) G. Andreetti, R. Ungaro, A. Pochini, J. Chem. Soc. Chem. Comm. (1979) 1005;
(b) C.D. Gutsche, Calixarenes, Royal Society of Chemistry, Cambridge, 1989;
(c) V. Bohmer, Angew. Chem. Int. Ed. 34 (1995) 713;
(d) A. Ikeda, S. Shinkai, Chem. Rev. 97 (1997) 1713;
(e) J. Rebeck Jr., Chem. Commun. (2000) 637;
(f) L. Pirondini, F. Bertolini, B. Cantadori, F. Ugozzoli, C. Massera, E. Dalcanale, Proc. Nat. Acad. Sci. 99 (2002) 4911;
(g) M.H.K. Ebbing, M.J. Villa, J.M. Valpuesta, P. Prados, J. de Mendoza, Proc. Nat. Acad Sci. 99 (2002) 4962.

[17] J.A.R. Navarro, E. Freisinger, B. Lippert, Eur. J. Inorg. Chem. (2000) 147.

[18] J.A.R. Navarro, M.B.L. Janik, E. Freisinger, B. Lippert, Inorg. Chem. 38 (1999) 426.

[19] J.A.R. Navarro, E. Freisinger, B. Lippert, Inorg. Chem. 39 (2000) 2301.

[20] J.A.R. Navarro, J.M. Salas, Chem. Comm. (2000) 235.

[21] E. Barea, J.A.R. Navarro, J.M. Salas, M. Willermann, B. Lippert, Chem. Eur. J. 9 (2003) 4414.

[22] S.Y. Yu, H. Huang, H.B. Liu, Z.N. Chen, R.B. Zhang, M. Fujita, Angew. Chem. Int. Ed. 42 (2003) 686.

[23] M.A. Galindo, M.A. Romero, J.A.R. Navarro, M. Quirós, Dalton Trans. (2004) 1563.

[24] M.A. Galindo, S. Galli, J.A.R. Navarro, M.A. Romero, Dalton Trans. (2004) 2780.

[25] L.C. Tabares, J.A.R. Navarro, J.M. Salas, Inorg. Chim. Acta 318 (2001) 166.
[26] (a) T. Ezuhara, K. Endo, K. Matsuda, Y. Aoyama, New J. Chem. 24 (2000) 609;
(b) T. Ezuhara, K. Endo, Y. Aoyama, J. Am. Chem. Soc. 121 (1999) 3279;
(c) T. Ezuhara, K. Endo, O. Hayashida, Y. Aoyama, New J. Chem. 22 (1998) 183.
[27] M. Quirós, Acta Crystallogr. C 50 (1994) 1236.
[28] N. Masciocchi, E. Corradi, M. Moret, G.A. Ardizzoia, A. Maspero, G. LaMonica, A. Sironi, Inorg. Chem. 36 (1997) 5648.
[29] N. Masciocchi, G.A. Ardizzoia, G. LaMonica, A. Maspero, A. Sironi, Angew. Chem. Int. Ed. Engl. 37 (1998) 3336.
[30] S. Galli, N. Masciocchi, E. Cariati, A. Sironi, E. Barea, M.A. Haj, J.A.R. Navarro, J.M. Salas, Chem. Mater., in press.
[31] J.A. Dean (Ed.), Large's Handbook of Chemistry, Section 9, 15th Ed., McGraw-Hill Inc., New York, NY, 1999.
[32] J.A.R. Navarro, E. Freisinger, B. Lippert, Inorg. Chem. 39 (2000) 1059.
[33] (a) M. Mascal, P.S. Fallon, A.S. Batsanov, B.R. Heynood, S. Champ, M. Colclough, J. Chem. Soc., Chem. Commun. (1995) 805;
(b) W.L. Jorgensen, J. Pranata, J. Am. Chem. Soc. 112 (1990) 2008;
(c) T.J. Murray, S.C. Zimmermann, J. Am. Chem. Soc. 114 (1992) 4010.
[34] (a) N. Masciocchi, G.A. Ardizzoia, A. Maspero, G. La Monica, A. Sironi, Inorg. Chem. 38 (1999) 3657;
(b) N. Masciocchi, G.A. Ardizzoia, S. Brenna, G. LaMonica, A. Maspero, S. Galli, A. Sironi, Inorg.Chem. 42 (2003) 6147.
[35] (a) N. Masciocchi, G.A. Ardizzoia, S. Brenna, F. Castelli, S. Galli, A. Maspero, A. Sironi, Chem. Commun. (2003) 2018;
(b) N. Masciocchi, S. Bruni, E. Cariati, F. Cariati, S. Galli, A. Sironi, Inorg. Chem. 40 (2001) 5897;
(c) N. Masciocchi, F. Castelli, P.M. Forster, M.M. Tafoya, A.K. Cheetham, Inorg. Chem. 42 (2003) 6147.
[36] N. Masciocchi, G.A. Ardizzoia, G. La Monica, A. Maspero, A. Sironi, Eur. J. Inorg. Chem. (2000) 2507.
[37] S.K. Kurtz, T.T. Perry, J. Appl. Phys. 39 (1968) 3798.
[38] N. Masciocchi, S. Galli, A. Sironi, E. Barea, J.A.R. Navarro, J.M. Salas, L. C. Tabares Chem. Mater. 15 (2003) 2153.
[39] E. Barea, J.A.R. Navarro, J.M. Salas, N. Masciocchi, S. Galli, A. Sironi, Inorg. Chem. 43 (2004) 473.
[40] M. O'Keeffe, B.G. Hyde, Crystal Structures I: Patterns and Symmetry, Minerallogical Society of America, Washington, 1996.
[41] E. Barea, M.A. Romero, J.A.R. Navarro, J.M. Salas, N. Masciocchi, S. Galli, A. Sironi, Inorg. Chem. 44 (2005) 1472.
[42] (a) L.C. Tabares, J.A.R. Navarro, J.M. Salas, J. Am. Chem. Soc. 123 (2001) 283;
(b) E. Barea, J.A.R. Navarro, J.M. Salas, N. Masciocchi, S. Galli, A. Sironi, J. Am. Chem. Soc. 125 (2004) 3015.
[43] E. Barea, J.A.R. Navarro, J.M. Salas, N. Masciocchi, S. Galli, A. Sironi, Polyhedron 22 (2003) 3051.
[44] E. Barea, J.A.R. Navarro, J.M. Salas, M. Quirós, Dalton Trans. (2005) 1743.